Few-Body Syst (2024) 65:79
https://doi.org/10.1007/s00601-024-01948-8

Thomas R. Richardson · **Immo C. Reis**

Radiative Corrections and the Renormalization Group for the Two-Nucleon Interaction in Effective Field Theory

Received: 14 June 2024 / Accepted: 22 July 2024
© The Author(s) 2024

Abstract We use a combination of effective field theory and the renormalization group to determine the impact of radiative corrections on the nucleon–nucleon potential and the binding energy of the deuteron. In order to do so, we present a modified version of pionless effective field theory inspired by earlier work in nonrelativistic quantum electrodynamics. The renormalization group improvement of the deuteron binding energy leads to a shift on the order of a few percent and is consistent with the experimental value. This work serves as a starting point for a dedicated study of radiative corrections in few-body systems relevant for precision tests of the Standard Model in an effective field theory framework.

1 Introduction

Modern experiments that rely on few-nucleon systems such as β-decay [1,2], μ-capture [3,4], and muonic atom spectroscopy [5–10] are reaching subpercent-level precision. Thus, these experiments can provide stringent tests for the Standard Model in low energy systems and possibly shed light on new physics. However, a correct interpretation of the experimental results requires a thorough theoretical understanding and delineation of the different effects involved.

In particular, these experiments are sensitive to radiative corrections from electrodynamics. In the context of muonic atom spectroscopy, a subset of these effects has been the subject of significant theoretical interest [11–13]. It is customary to include radiative corrections through finite nuclear size effects and the exchange of two or more photons between the nucleus and the bound muon. The nuclear wavefunctions and currents, however, only include electromagnetic effects implicitly by fitting the parameters of the nuclear Hamiltonian and currents to data. Because of this, there is no way to distill how much of an observable comes from quantum chromodynamics (QCD) as opposed to electroweak interactions.

In the case of β-decays, this topic has received renewed interest in recent years with respect to single-neutron β-decay [14–21]. Interestingly, Ref. [15] finds a percent level shift in the nucleon axial coupling g_A due to radiative corrections that shifts the lattice QCD determination of g_A closer to the more precise experimental value. This represents a significant step towards disentangling the myriad of effects involved in neutron β decay in terms of Standard Model parameters.

The goal of this work is to begin bridging the gap in few-nucleon systems with effective field theory (EFT) techniques. We use a combination of pionless effective field theory ($\text{EFT}_{\not\pi}$) [22–30] and the

Thomas R. Richardson, Immo C. Reis have contributed equally to this work.

T. R. Richardson (✉) · I. C. Reis
Institut für Kernphysik and PRISMA+ Cluster of Excellence, Johannes Gutenberg-Universität, 55128 Mainz, Germany
E-mail: richardt@uni-mainz.de

I. C. Reis
E-mail: imreis@students.uni-mainz.de

Published online: 05 August 2024

velocity renormalization group (vRG) [31] developed for nonrelativistic QED (NRQED) [32]. This theory is valid for momenta $p \ll m_\pi$, where m_π is the pion mass, which is in the regime relevant for many of these experiments. Certain aspects of this work can also be applied in chiral EFT [30,33–36], which has a larger radius of convergence. On the other hand, the entire framework can immediately be applied in an EFT for halo nuclei [30,37–39] with trivial modifications.

In this work, we use the renormalization group to sum the leading logarithm series in α, where $\alpha = e^2/4\pi$ is the fine structure constant, into the coefficients of the neutron-proton potential. The running couplings that follow from the vRG equations can in principle be embedded in *ab initio* calculations using few- or many-body methods. The electromagnetic renormalization of this potential will generate isospin breaking contributions in the electroweak processes already described (see, e.g., Refs. [40–43] in the context of nuclear β-decays).

To illustrate the impact of the running induced by the radiative corrections, we use renormalization group improved perturbation theory to calculate the deuteron binding energy and compare the result to the fixed order calculation. In order to generate numerical results, the vRG equations require a boundary condition to fix the final value of low energy coefficients (LECs). Ideally, the LECs in a nuclear EFT in the absence of electroweak effects would be determined by lattice QCD rather than data. However, available few-nucleon lattice calculations have greater than physical m_π and the uncertainties are quite large. In the meantime, we make use of the scattering parameters of the phenomenological Argonne $v18$ (AV18) potential without electromagnetic interactions found in Table VIII of Ref. [44] (also see Ref. [45]). Here, we find that vRG improvement drives a percent level shift in the deuteron binding energy. This observation is consistent with the AV18 potential, but it recasts the impact of electromagnetic corrections to the nucleon-nucleon (NN) interactions in terms of a modern EFT with the full machinery of the renormalization group.

2 Reorganizing Pionless Effective Field Theory

Now, we recast $\text{EFT}_{\not\pi}$ in the language of velocity NRQED (vNRQED) [31]. In $\text{EFT}_{\not\pi}$ it is typical to count powers of the momentum p, but in NRQED powers of velocity $v = p/M_N$, where M_N is the nucleon mass, are counted. However, some care is needed in judging the scaling of electromagnetic interactions relative to the strong NN interaction; we revisit this at the end of this section. The relevant (energy, momentum) scales are then expressed as hard (m_π, m_π), soft $(M_N v, M_N v)$, ultrasoft $(M_N v^2, M_N v^2)$, and potential $(M_N v^2, M_N v)$. Power counting issues are avoided by splitting the photon into multiple modes describing the soft and ultrasoft regions and multipole expanding the ultrasoft modes [46–51]. The potential photons can be integrated out because they are far off-shell; their effects are encoded in the coefficients of four-nucleon operators.

After performing a nonrelativistic reduction, the four-momentum of the nucleon is decomposed as

$$P = (0, \mathbf{p}) + (k_0, \mathbf{k}) \,, \tag{1}$$

where $\mathbf{p} \sim M_N v$ is the soft component of the momentum and $k \sim M_N v^2$ is the residual four-momentum on the ultrasoft scale. The on-shell condition becomes $k_0 = \mathbf{p}^2/2M_N$. The nucleon field is now written as $N_{\mathbf{p}}(x)$ where $\mathbf{p}$ is a soft label, x is the Fourier conjugate of the residual momentum k, and N is an isodoublet of the proton and neutron.

The photon field is also split into a soft field $A^\mu_p(k)$ with soft label four-momentum p and a residual four-momentum k and an ultrasoft field A^μ. Conservation of energy excludes interactions of the type $A_q N^\dagger_{\mathbf{p}} N_{\mathbf{p}}$, i.e., only vertices with two soft photon lines are allowed. The kinetic term of the photon field is split into

$$\mathcal{L} \supset -\frac{1}{4} F_{\mu\nu} F^{\mu\nu} + \sum_p \left| p^\mu A^\nu_p - p^\nu A^\mu_p \right|^2 \,, \tag{2}$$

where the field strength tensor $F_{\mu\nu}$ contains only ultrasoft photons.

Reparameterization invariance implies that derivatives acting on the nucleon fields appear in the combination $i\mathbf{p} + \mathbf{D}$, where $\mathbf{p}$ acts on the soft label and $\mathbf{D}$ is a covariant derivative acting on the residual piece of the nucleon field. In the kinetic term for the nucleon, the term $(\mathbf{p} - i\mathbf{D})^2$ should be expanded, which is equivalent to the multipole expansion, and only the $\mathbf{p}^2$ should be kept in the leading order propagator. Therefore, the nucleon propagator will be

$$S(k_0, \mathbf{p}) = \frac{i}{k_0 - \frac{\mathbf{p}^2}{2M_N} + i\epsilon} \,. \tag{3}$$

Terms containing factors of $\mathbf{p}\cdot\nabla$ or ∇^2 are treated as perturbations.

While EFT$_{\not\pi}$ is usually formulated in an isospin basis, we find it more convenient to study the ultrasoft renormalization of the potential in terms of physical neutron and proton fields n and p, respectively. The LECs can of course be translated into the isospin basis after the renormalization has been carried out. In this basis, the proton–neutron potential is written as

$$V_{pn} = \sum_{v=-1}\sum_{\mathbf{p}',\mathbf{p}} V^{(v,pn)}_{abcd}(\mathbf{p}',\mathbf{p})\, p^\dagger_{\mathbf{p}',a}\, p_{\mathbf{p},b}\, n^\dagger_{-\mathbf{p}',c}\, n_{-\mathbf{p},d}\,, \tag{4}$$

where v tracks the order in the velocity expansion of each coefficient, and a, b, c, and d are spin indices for the neutron and proton fields. The leading order (LO), next-toleading order (NLO), and next-to-next-to-leading order (N^{2}LO) potential coefficients in the S-wave are given by

$$V^{(-1,pn)}_{abcd} = C^{(^3S_1)}_{0,pn} P^{(1)}_{ab,cd} + C^{(^1S_0)}_{0,pn} P^{(0)}_{ab,cd}\,, \tag{5}$$

$$V^{(0,pn)}_{abcd} = \frac{1}{2}\left(\mathbf{p}'^2+\mathbf{p}^2\right)\left[C^{(^3S_1)}_{2,pn} P^{(1)}_{ab,cd} + C^{(^1S_0)}_{2,pn} P^{(0)}_{ab,cd}\right]\,, \tag{6}$$

$$V^{(1,pn)}_{abcd} = \frac{1}{4}\left(\mathbf{p}'^2+\mathbf{p}^2\right)^2\left[C^{(^3S_1)}_{4,pn} P^{(1)}_{ai,bj} + C^{(^1S_0)}_{4,pn} P^{(0)}_{ab,cj}\right]\,, \tag{7}$$

where the projection operators are given by

$$P^{(1)}_{ab,cd} = \frac{1}{4}\left(3\delta_{ab}\delta_{cd} + \sigma^i_{ab}\sigma^i_{cd}\right)\,, \tag{8}$$

$$P^{(0)}_{ab,cd} = \frac{1}{4}\left(\delta_{ab}\delta_{cd} - \sigma^i_{ab}\sigma^i_{cd}\right)\,. \tag{9}$$

Note that our definition of C_4 is a linear combination of $C_4+\tilde{C}_4$ that appears in the literature (see for example Refs. [26–28]). The $V^{(0)}$ potential should also be supplemented with a correction to the Coulomb potential that arises from a potential photon coupled to the proton charge and the neutron charge radius as well as a term that couples the neutron and proton magnetic moments; however, these terms are also suppressed by a factor of α bringing the overall sizes to $O(\alpha v^0)$. Therefore, the velocity power counting suggests that these contributions are higher order than what we will consider.

The neutron-neutron potentials have an identical structure with respect to the purely strong interactions. The part of the potential that arises from potential photon exchange is $O(\alpha v^2)$. The strong part of the proton–proton potential is also identical to the proton–neutron potential. However, we have to add the Coulomb potential to the leading order term.

$$V^{(-1,pp)}_{abcd} \supset \sum_{\mathbf{p}',\mathbf{p}} \frac{4\pi\alpha}{(\mathbf{p}'-\mathbf{p})^2}\delta_{ab}\delta_{cd}. \tag{10}$$

In the remainder of this work we will only consider the proton–neutron channel, so we only retain V_{pn} from Eq. (4). All together, the Lagrangian we will work with is

$$\begin{aligned}\mathcal{L} = &\sum_{\mathbf{p}} N^\dagger_{\mathbf{p}}\left(iD_0 - \frac{(\mathbf{p}-i\mathbf{D})^2}{2M_N}\right)N_{\mathbf{p}} - \frac{1}{4}F_{\mu\nu}F^{\mu\nu} + \sum_{\mathbf{p}}\left|p^\mu A^\nu_p - p^\nu A^\mu_p\right|^2 - V_{pn}\\ &- \frac{4\pi\alpha}{2M_N}\sum_{q,q',\mathbf{p},\mathbf{p}'}\mathbf{A}_{q'}\cdot\mathbf{A}_q N^\dagger_{\mathbf{p}'} Q N_{\mathbf{p}} + \frac{e}{2M_N}\epsilon^{ijk}\left(\nabla^j A^k\right)\sum_{\mathbf{p}} N^\dagger_{\mathbf{p}}\sigma^i\left[\kappa_0+\kappa_1\tau^3\right]N_{\mathbf{p}}\,,\end{aligned} \tag{11}$$

where we have reverted to the nucleon isodoublet $N_{\mathbf{p}}$ in the single-nucleon terms to condense the notation, $Q=(\mathbb{1}+\tau_3)/2$ is the nucleon charge matrix, and V_{pn} is the neutron-proton potential defined in terms of neutron and proton fields in Eq. (4) with coefficients from Eqs. (5)–(7).

Counting powers of velocity in Feynman diagrams is fairly straightforward. Nucleon and soft photon propagators count as $1/v^2$ while ultrasoft photon propagators count as $1/v^4$. The purely NN potentials follow the standard power counting of EFT$_{\not\pi}$ where $Q\sim M_N v$ [23,24]. Finally, a soft loop has an integration measure that scales as v^4, a potential loop scales as v^5, and an ultrasoft loop scales as v^8.

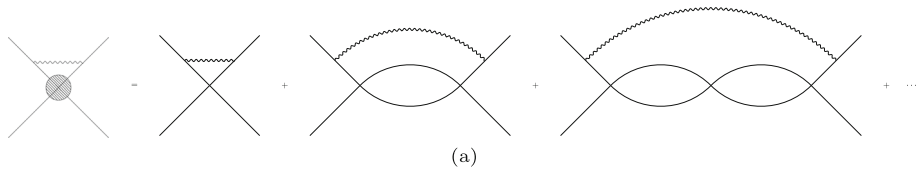

Fig. 1 $O(\alpha/v)$ diagrams that contribute to the anomalous dimension of the potential

In order to implement the vRG, we determine the $O(\alpha/v)$ counterterms and obtain the soft and ultrasoft anomalous dimensions from [31,52]

$$\mu_U \frac{dV}{d\mu_U} = \gamma_U \,, \tag{12}$$

$$\mu_S \frac{dV}{d\mu_S} = \gamma_S \,, \tag{13}$$

where μ_S is the scale introduced in dimensional regularization for the potentials and soft interactions and μ_U is the scale introduced for the ultrasoft interactions. Through these scales we introduce the subtaction velocity ν as $\mu_S = M_N \nu$ and $\mu_U = M_N \nu^2$ so that the vRG equation is

$$\nu \frac{dV}{d\nu} = \gamma_S + 2\gamma_U \,. \tag{14}$$

In NRQED, this procedure is fairly easy because the fine structure constant α does not run and the LO Coulomb potential is not renormalized [53]. Moreover, the α and v expansions are identical since the average velocity in a Coulomb bound state is $O(\alpha)$. As we will see below, because the α and v expansions are not strictly linked in the nuclear EFT and because α runs due to the fact that the electron mass is not integrated out of the theory, there is a much richer structure that arises from the vRG.

Before proceeding to the calculation of the anomalous dimensions, we comment further on the power counting in this EFT. As previously mentioned, the v and α expansions are not identical as they are in pure NRQED. However, we can estimate the relative importance of $O(\alpha)$ corrections to the strong sector. The typical relative momentum in the deuteron is $p \sim 50$ MeV, so that the the expansion in the purely strong sector is in powers of $Q = p/m_\pi$ which is roughly $1/3$. For $\alpha \sim 1/137$, a conservative estimate in this regime suggests $\alpha \sim Q^4$. Thus, through N^{2}LO in the potential sector, we can safely neglect the finite contributions from the diagrams when we calculate the binding energy of the deuteron below and encode the effects from radiative correction in the running couplings via the solutions of the vRG equations. We expect that these contributions should be included explicitly around next-to-next-to-next-to-leading order (N^{3}LO). Indeed, these contributions are already probed through the variation of the subtraction velocity. For other processes such as proton–proton fusion where the typical momentum or velocity is somewhat smaller, the explicit radiative corrections will enter at even lower orders.

In the remainder of this work, we will focus mainly on the neutron-proton sector at $O(\alpha/v)$. The neutron–neutron potential will be renormalized at higher orders in the v expansion. Renormalizing the proton–proton potential is much more involved. The Coulomb interaction will generate a nonzero soft anomalous dimension for C_0 [54] leading to a faster running. Thus, we expect the vRG to lead to interesting results in this channel.

3 Renormalization

The renormalization procedure in this theory is reminiscent of the role of radiation pions in EFT [55]. However, there are several important differences. First, we can treat both ultraviolet and infrared divergences in dimensional regularization, which simplifies the loop integrals. Second, the neutron has no coupling to A_0 photons at the order we are working.

With this set-up, the basic topologies that renormalize the potential are shown in Fig. 1. In Feynman gauge, the dominant contribution, which is $O(\alpha/v)$, comes from an A_0 photon coupled to the proton on both the incoming and outgoing lines with insertions of the C_0 potential. Inside the ultrasoft loop, an arbitrary number of NN bubbles with only C_0 vertices will contribute at the same order; therefore, the internal bubble diagrams must be summed to all orders.

This infinite sum of diagrams often makes explicit renormalization of the series intractable. The argument in the case of radiation pions is that the bubble sum should be performed before the ultrasoft integration [55]. However, it should really be understood that the *finite* parts of the bubbles are being summed, i.e., all divergences are canceled by the appropriate counterterms and the remainder is resummed. In this case, we can actually perform this renormalization to all orders in C_0.

In the bubble series, each graph is divergent. However, each graph with an odd number of *NN* bubbles is ultraviolet finite and the divergence is purely infrared. Each graph with an even number of *NN* bubbles has both ultraviolet and infrared divergences which must be separated. Specifically, a graph with $l = 2j$ bubbles, where j is an integer, requires a counterterm that renormalizes the $2j$-derivative potential. For example, the diagram with 0 *NN* bubbles renormalizes the $V^{(-1)}$ potential while the diagram with 2 *NN* bubbles renormalizes the $V^{(0)}$ potential. For arbitrary j, the appropriate counterterm in minimal subtraction is

$$\delta C_{2j} = \frac{\alpha C_0}{2\pi}\left(\frac{iM_N C_0}{4\pi}\right)^{2j}\frac{1}{j+1}\frac{1}{\epsilon}\,. \tag{15}$$

For the LO potential, we find $\gamma_{S,0} = 0$ while

$$\gamma_{U,0} = \frac{1}{2\pi}\alpha(M_N\nu^2)C_0\,, \tag{16}$$

which leads to the vRG equation

$$\nu\frac{dC_0}{d\nu} = \frac{1}{\pi}\alpha(M_N\nu^2)C_0. \tag{17}$$

For $j \geq 1$, we find

$$\gamma_{S,2j} \supset \frac{\alpha}{\pi}\frac{2j}{j+1}C_0\left(\frac{iM_N C_0}{4\pi}\right)^{2j}\,, \tag{18}$$

$$\gamma_{U,2j} \supset \frac{\alpha}{2\pi}\frac{3+4j}{j+1}C_0\left(\frac{iM_N C_0}{4\pi}\right)^{2j}\,. \tag{19}$$

There is also a contribution to the ultrasoft anomalous dimension of the $2j$-derivative operator from an insertion of the operator itself into the one-loop diagram, i.e., the first diagram on the right hand side of Fig. 1. This contribution is identical to that for C_0 though only with C_{2j} appearing instead. Dressing the potential vertex with additional C_0 interactions leads to diagrams of the same order in v, which will also generate contributions to the soft anomalous dimension of higher-derivative operators. However, these contributions are still be suppressed relative to the anomalous dimensions presented here. Retaining only the leading contribution to the anomalous dimension leads to the vRG equation

$$\nu\frac{dC_{2j}}{d\nu} = \frac{\alpha}{\pi}\frac{3+6j}{j+1}C_0\left(\frac{iM_N C_0}{4\pi}\right)^{2j}\,. \tag{20}$$

Integrating the vRG equation gives

$$C_0(\nu) = C_0\left(\frac{m_\pi}{M_N}\right)\left(\frac{\alpha(M_N\nu^2)}{\alpha(m_\pi^2/M_N)}\right)^{3/4}\,, \tag{21}$$

$$C_2(\nu) = C_2\left(\frac{m_\pi}{M_N}\right) - \frac{3}{2}\left(\frac{M_N}{4\pi}\right)^2 C_0^3\left(\frac{m_\pi}{M_N}\right)\left[\left(\frac{\alpha(M_N\nu^2)}{\alpha(m_\pi^2/M_N)}\right)^{9/4} - 1\right]\,, \tag{22}$$

$$C_4(\nu) = C_4\left(\frac{m_\pi}{M_N}\right) + \left(\frac{M_N}{4\pi}\right)^4 C_0^5\left(\frac{m_\pi}{M_N}\right)\left[\left(\frac{\alpha(M_N\nu^2)}{\alpha(m_\pi^2/M_N)}\right)^{15/4} - 1\right]\,. \tag{23}$$

In Fig. 2, we show the running of the potential LECs normalized as

$$\hat{C}_{2j}(\nu) = \frac{C_{2j}(\nu)}{C_{2j}(m_\pi/M_N)}\,, \tag{24}$$

where the normalization condition is discussed below in Eqs. (32) through Eq. (37). The zero-derivative potential runs very slowly while $\hat{C}_2$ differs by several percent from its value at the hard scale when $\nu < 0.06$. The running of $\hat{C}_4$ is significantly faster; it changes by nearly 50% when $\nu \sim 0.06$

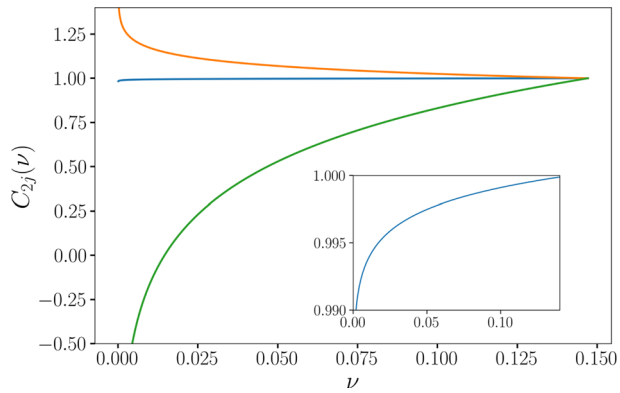

Fig. 2 The running of the potential coefficients. The blue line is the running of $\hat{C}_0$, the orange line is the running of $\hat{C}_2$, and the green line is the running of $\hat{C}_4$

4 Impact in the Deuteron

The two-point correlation function for the deuteron is given by [56]

$$G(\bar{E}) = \frac{\Sigma(\bar{E})}{1 + iC_0\Sigma(\bar{E})}\,, \tag{25}$$

where Σ is the self-energy of the deuteron and consists of irreducible diagrams in the sense that they do not fall apart when cut at a C_0 vertex. The self-energy is expanded as

$$\Sigma(\bar{E}) = \Sigma_1(\bar{E}) + \Sigma_2(\bar{E}) + \Sigma_3(\bar{E}) + \cdots \tag{26}$$

where $\bar{E}$ is the center-of-mass energy and the dots stand for higher order terms. The subscript indicates the order of the contribution in the velocity expansion.

On one hand, the two-point function has the form

$$G(\bar{E}) = \frac{i\tilde{Z}}{\bar{E} + \tilde{B}}\,, \tag{27}$$

where $\tilde{Z}$ and $\tilde{B}$ are the wave-function renormalization and binding energy in the full theory, respectively. The perturbative corrections lead to shifts in the wave function renormalization $\tilde{Z} = Z + \delta Z$ and the binding energy $B = B + \delta B$, where Z and B are the LO results for the wave-function renormalization and binding energy, respectively. Expanding the two-point function leads to

$$G(\bar{E}) = \frac{i\,(Z + \delta Z)}{\bar{E} + B}\left[1 - \frac{\delta B}{\bar{E} + B} + \cdots\right]. \tag{28}$$

The energy shift δB can now be identified as the coefficient of $-iZ/(\bar{E} + B)^2$ (see for instance Ref. [57]).

On the other hand, the two-point function can be expanded as

$$G(\bar{E}) = \frac{\Sigma_1}{1 + iC_0\Sigma_1} + \frac{(-iC_2)(M_N\bar{E})\Sigma_1^2}{(1 + iC_0\Sigma_1)^2} + \frac{(-iC_4)(M_N\bar{E})^2\Sigma_1^2}{(1 + iC_0\Sigma_1)^2} - \frac{C_2^2(M_N\bar{E})^2\Sigma_1^3}{(1 + iC_0\Sigma_1)^3} + \cdots\,, \tag{29}$$

where each coupling is a function of the subtraction velocity ν. In the sector of the theory with only potential terms, this is equivalent to time independent perturbation theory in ordinary quantum mechanics. Thus, the shift in the binding energy can be obtained by inserting the LO expression of the self-energy and manipulating the denominators of the second and third terms until reaching the form of Eq. (28). The last term requires more care. This term corresponds to a second-order perturbation theory calculation with the C_2 interaction, so we must explicitly separate the contribution of the deuteron in this term. This is equivalent to calculating

$$\langle\psi|\,V^{(0)}\frac{1}{E - H}V^{(0)}\,|\psi\rangle - \frac{1}{E + B}\left|\langle\psi|\,V^{(0)}\,|\psi\rangle\right|^2\,, \tag{30}$$

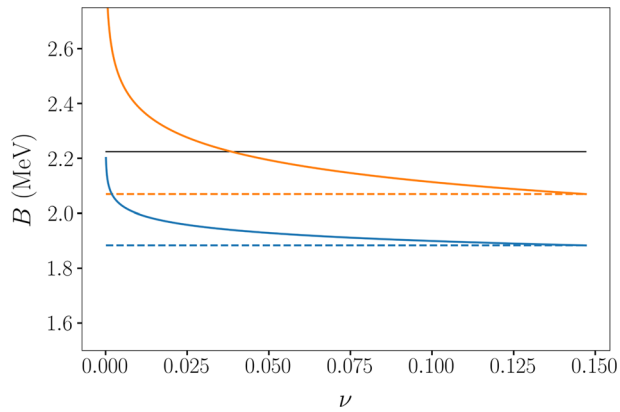

Fig. 3 The deuteron binding energy as a function of the subtraction velocity. The solid black line is the experimental value. The blue (orange) dashed line is the fixed order NLO (N^2LO) result while the blue (orange) solid line is the renormalization group improved NLO (N^2LO) result

where H is the full LO Hamiltonian containing $V^{(-1)}$. All together the binding energy to N^2LO is

$$B = \frac{1}{M_N}\left(\frac{4\pi}{M_N C_0}\right)^2 + \frac{1}{2\pi}C_2\left(\frac{4\pi}{M_N C_0}\right)^5 + \frac{7}{16\pi^2}M_N C_2^2\left(\frac{4\pi}{M_N C_0}\right)^8 - \frac{1}{2\pi}C_4\left(\frac{4\pi}{M_N C_0}\right)^7 \tag{31}$$

We use the scattering length and effective range of the AV18 potential [44] without the electromagnetic interaction as the boundary value (i.e. at $\nu = m_\pi/M_N$) of the vRG equations. Electromagnetic corrections to the shape parameter P are also expected to be small, so we use the Nijmegen value [58]. In the deuteron channel, these are

$$a_{np} = 5.402\ \text{fm}\,, \tag{32}$$
$$r_{np} = 1.752\ \text{fm}\,, \tag{33}$$
$$P_{np} = 0.040\ \text{fm}^{-3}\,. \tag{34}$$

The LECs at $\nu = m_\pi/M_N$ are given in terms of these parameters according to

$$C_0(m_\pi/M_N) = \frac{4\pi a_{np}}{M_N}\,, \tag{35}$$
$$C_2(m_\pi/M_N) = \frac{4\pi}{M_N}\frac{a_{np}^2 r_{np}}{2}\,, \tag{36}$$
$$C_4(m_\pi/M_N) = \frac{4\pi}{M_N}a_{np}^3\left(\frac{1}{4}r_{np}^2 + \frac{P_{np}}{a_{np}}\right)\,. \tag{37}$$

The result for the deuteron binding energy at NLO and N^2LO is shown in Fig. 3. First, we can compare the values of the renormalization group improved binding energies at each order in the EFT to the values at the hard scale $\nu = m_\pi/M_N$. When the subtraction velocity is $\nu \approx 0.04$ (corresponding to momenta around 38 MeV), there is a shift in the binding energy of about 2.5% at NLO. At N^2LO, the improvement shifts the binding energy by about 7%. Moreover, the improvement at N^2LO causes the predicted binding energy to intersect the experimental value $B = 2.224575$ MeV around $\nu \approx 0.04$. Second, we can compare the shift in the predicted binding energy at different orders in the EFT for the same subtraction velocities. At the hard scale $\nu = m_\pi/M_N$, the binding energy at N^2LO is about 10% larger than the result at NLO. At $\nu \approx 0.04$, the N^2LO is around 17% larger than the NLO result.

5 Summary

In this work, we have performed an analysis of the role of radiative corrections in the *NN* system. Using EFT techniques helps to organize the role of different strong and electromagnetic effects in a systematic expansion.

Additionally, we performed the first direct application of the vRG in a nuclear EFT. This allows us to sum the leading logarithm series into the potential coefficients. We then provided evidence that the vRG generates a percent level shift in the binding energy of the deuteron. It is possible that similar corrections will play an important role in other light nuclei. This prediction will be more robust when reliable *NN* observables can be calculated in lattice QCD at the physical pion mass in order to match the couplings of this EFT.

The ultrasoft renormalization of the leading order potential in chiral EFT can be analyzed with similar techniques. First, the one-pion exchange potential will be written as a four-fermion operator where the LEC is determined by the axial coupling g_A and the pion decay constant F_π at the breakdown scale of chiral EFT in the absence of electroweak effects. Then the tree-level potential will be dressed with an ultrasoft photon that leads to an anomalous dimension similar to Eq. (16), only C_0 is replaced by $(g_A/F_\pi)^2$ up to a factor of 2. Also, the contact potential proportional to C_0 will acquire a nonzero soft anomalous dimension driven by pion exchange. Renormalizing the potential at higher orders will be significantly more difficult.

The running couplings obtained in this work can also be incorporated into other $\text{EFT}_{\not\pi}$ calculations or in *ab initio* methods for nuclear physics that make use of $\text{EFT}_{\not\pi}$ potentials derived with dimensional regularization. In this way, this renormalization group study can impact a variety of theoretical work relevant for ongoing experiments including β-decay, μ-capture, and muonic atom spectroscopy.

Acknowledgements We would like to thank Sonia Bacca, Wouter Dekens, Aneesh Manohar, Matthias Schindler, and Roxanne Springer for interesting discussions. This work was supported in part by the Deutsche Forschungsgemeinschaft (DFG) through the Cluster of Excellence "Precision Physics, Fundamental Interactions, and Structure of Matter" (PRISMA$^+$ EXC 2118/1) funded by the DFG within the German Excellence Strategy (Project ID 390831469).

Open Access This article is licensed under a Creative Commons Attribution 4.0 International License, which permits use, sharing, adaptation, distribution and reproduction in any medium or format, as long as you give appropriate credit to the original author(s) and the source, provide a link to the Creative Commons licence, and indicate if changes were made. The images or other third party material in this article are included in the article's Creative Commons licence, unless indicated otherwise in a credit line to the material. If material is not included in the article's Creative Commons licence and your intended use is not permitted by statutory regulation or exceeds the permitted use, you will need to obtain permission directly from the copyright holder. To view a copy of this licence, visit http://creativecommons.org/licenses/by/4.0/.

Author Contribution All authors wrote the main manuscript text and reviewed it. T.R.R. prepared all figures.

Data Availability No datasets were generated or analysed during the current study.

Declarations

Competing interests The authors declare no competing interests.

References

1. D. Počanić, R. Alarcon, L.P. Alonzi, S. Baeßler, S. Balascuta, J.D. Bowman, M.A. Bychkov, J. Byrne, J.R. Calarco, V. Cianciolo, C. Crawford, E. Frlež, M.T. Gericke, G.L. Greene, R.K. Grzywacz, V. Gudkov, F.W. Hersman, A. Klein, J. Martin, S.A. Page, A. Palladino, S.I. Penttilä, K.P. Rykaczewski, W.S. Wilburn, A.R. Young, G.R. Young, Nab: Measurement principles, apparatus and uncertainties. Nucl. Instrum. Methods Phys. Res., Sect. A **611**(2), 211–215 (2009). https://doi.org/10.1016/j.nima.2009.07.065
2. D. Dubbers, H. Abele, S. Baeßler, B. Märkisch, M. Schumann, T. Soldner, O. Zimmer, A clean, bright, and versatile source of neutron decay products. Nucl. Instrum. Methods Phys. Res. Sect. A **596**(2), 238–247 (2008). https://doi.org/10.1016/j.nima.2008.07.157
3. V.A. Andreev, R.M. Carey, V.A. Ganzha, A. Gardestig, T. Gorringe, F.E. Gray, D.W. Hertzog, M. Hildebrandt, P. Kammel, B. Kiburg, S. Knaack, P.A. Kravtsov, A.G. Krivshich, K. Kubodera, B. Lauss, K.R. Lynch, E.M. Maev, O.E. Maev, F. Mulhauser, F. Myhrer, C. Petitjean, G.E. Petrov, R. Prieels, G.N. Schapkin, G.G. Semenchuk, M.A. Soroka, V. Tishchenko, A.A. Vasilyev, A.A. Vorobyov, M.E. Vznuzdaev, P. Winter, Muon Capture on the Deuteron: The MuSun Experiment (2010). arXiv:1004.1754
4. P. Kammel, MuSun-Muon capture on the deuteron. SciPost Phys. Proc. **5**, 18 (2021). https://doi.org/10.21468/SciPostPhysProc.5.018
5. A. Antognini, S. Bacca, A. Fleischmann, L. Gastaldo, F. Hagelstein, P. Indelicato, A. Knecht, V. Lensky, B. Ohayon, V. Pascalutsa, N. Paul, R. Pohl, F. Wauters, Muonic-atom spectroscopy and impact on nuclear structure and precision QED theory (2022). arXiv:2210.16929
6. A. Antognini, F. Nez, K. Schuhmann, F.D. Amaro, F. Biraben, J.M.R. Cardoso, D.S. Covita, A. Dax, S. Dhawan, M. Diepold, L.M.P. Fernandes, A. Giesen, A.L. Gouvea, T. Graf, T.W. Hänsch, P. Indelicato, L. Julien, C.Y. Kao, P. Knowles, F. Kottmann, E.O. Le Bigot, Y.W. Liu, J.A.M. Lopes, L. Ludhova, C.M.B. Monteiro, F. Mulhauser, T. Nebel, P. Rabinowitz, J.M.F. Dos Santos, L.A. Schaller, C. Schwob, D. Taqqu, J.F.C.A. Veloso, J. Vogelsang, R. Pohl, Proton structure from the measurement

of 2S–2P transition frequencies of muonic hydrogen. Science **339**(6118), 417–420 (2013). https://doi.org/10.1126/science.1230016
7. R. Pohl, F. Nez, L.M.P. Fernandes, F.D. Amaro, F. Biraben, J.M.R. Cardoso, D.S. Covita, A. Dax, S. Dhawan, M. Diepold, A. Giesen, A.L. Gouvea, T. Graf, T.W. Hänsch, P. Indelicato, L. Julien, P. Knowles, F. Kottmann, E.O. Le Bigot, Y.W. Liu, J.A.M. Lopes, L. Ludhova, C.M.B. Monteiro, F. Mulhauser, T. Nebel, P. Rabinowitz, J.M.F. Dos Santos, L.A. Schaller, K. Schuhmann, C. Schwob, D. Taqqu, J.F.C.A. Veloso, A. Antognini, The CREMA collaboration, laser spectroscopy of muonic deuterium. Science **353**(6300), 669–673 (2016). https://doi.org/10.1126/science.aaf2468
8. R. Pohl, A. Antognini, F. Nez, F.D. Amaro, F. Biraben, J.M.R. Cardoso, D.S. Covita, A. Dax, S. Dhawan, L.M.P. Fernandes, A. Giesen, T. Graf, T.W. Hänsch, P. Indelicato, L. Julien, C.Y. Kao, P. Knowles, E.O. Le Bigot, Y.W. Liu, J.A.M. Lopes, L. Ludhova, C.M.B. Monteiro, F. Mulhauser, T. Nebel, P. Rabinowitz, J.M.F. dos Santos, L.A. Schaller, K. Schuhmann, C. Schwob, D. Taqqu, J.F.C.A. Veloso, F. Kottmann, The size of the proton. Nature **466**(7303), 213–216 (2010). https://doi.org/10.1038/nature09250
9. J.J. Krauth, K. Schuhmann, M.A. Ahmed, F.D. Amaro, P. Amaro, F. Biraben, T.L. Chen, D.S. Covita, A.J. Dax, M. Diepold, L.M.P. Fernandes, B. Franke, S. Galtier, A.L. Gouvea, J. Götzfried, T. Graf, T.W. Hänsch, J. Hartmann, M. Hildebrandt, P. Indelicato, L. Julien, K. Kirch, A. Knecht, Y.W. Liu, J. Machado, C.M.B. Monteiro, F. Mulhauser, B. Naar, T. Nebel, F. Nez, J.M.F. dos Santos, J.P. Santos, C.I. Szabo, D. Taqqu, J.F.C.A. Veloso, J. Vogelsang, A. Voss, B. Weichelt, R. Pohl, A. Antognini, F. Kottmann, Measuring the α-particle charge radius with muonic helium-4 ions. Nature **589**(7843), 527–531 (2021). https://doi.org/10.1038/s41586-021-03183-1
10. T.C. Collaboration, K. Schuhmann, L.M.P. Fernandes, F. Nez, M.A. Ahmed, F.D. Amaro, P. Amaro, F. Biraben, T.L. Chen, D.S. Covita, A.J. Dax, M. Diepold, B. Franke, S. Galtier, A.L. Gouvea, J. Götzfried, T. Graf, T.W. Hänsch, M. Hildebrandt, P. Indelicato, L. Julien, K. Kirch, A. Knecht, F. Kottmann, J.J. Krauth, Y.W. Liu, J. Machado, C.M.B. Monteiro, F. Mulhauser, B. Naar, T. Nebel, J.M.F. dos Santos, J.P. Santos, C.I. Szabo, D. Taqqu, J.F.C.A. Veloso, A. Voss, B. Weichelt, A. Antognini, R. Pohl, The helion charge radius from laser spectroscopy of muonic helium-3 ions (2023). arXiv: 2305.11679
11. A. Antognini, F. Hagelstein, V. Pascalutsa, The proton structure in and out of muonic hydrogen. Ann. Rev. Nucl. Part. Sci. **72**(1), 389–418 (2022). https://doi.org/10.1146/annurev-nucl-101920-024709
12. C. Ji, S. Bacca, N. Barnea, O.J. Hernandez, N. Nevo-Dinur, Ab initio calculation of nuclear structure corrections in muonic atoms. J. Phys. G Nucl. Part. Phys. **45**(9), 093002 (2018). https://doi.org/10.1088/1361-6471/aad3eb
13. K. Pachucki, V. Lensky, F. Hagelstein, S.S.L. Muli, S. Bacca, R. Pohl, Comprehensive theory of the Lamb shift in light muonic atoms (2023). arXiv: 2212.13782
14. S. Ando, H.W. Fearing, V. Gudkov, K. Kubodera, F. Myhrer, S. Nakamura, T. Sato, Neutron beta decay in effective field theory. Phys. Lett. B **595**(1–4), 250–259 (2004). https://doi.org/10.1016/j.physletb.2004.06.037
15. V. Cirigliano, J. de Vries, L. Hayen, E. Mereghetti, A. Walker-Loud, Pion-induced radiative corrections to neutron beta-decay. Phys. Rev. Lett. **129**(12), 121801 (2022). https://doi.org/10.1103/PhysRevLett.129.121801
16. C.Y. Seng, M. Gorchtein, M.J. Ramsey-Musolf, Dispersive evaluation of the inner radiative correction in neutron and nuclear β-decay. Phys. Rev. D **100**(1), 013001 (2019). https://doi.org/10.1103/PhysRevD.100.013001
17. C.Y. Seng, M. Gorchtein, H.H. Patel, M.J. Ramsey-Musolf, Reduced hadronic uncertainty in the determination of V_{ud}. Phys. Rev. Lett. **121**(24), 241804 (2018). https://doi.org/10.1103/PhysRevLett.121.241804
18. V. Cirigliano, W. Dekens, E. Mereghetti, O. Tomalak, Effective field theory for radiative corrections to charged-current processes I: Vector coupling. Phys. Rev. D **108**(5), 053003 (2023). https://doi.org/10.1103/PhysRevD.108.053003
19. A. Czarnecki, W.J. Marciano, A. Sirlin, Radiative corrections to neutron and nuclear beta decays revisited. Phys. Rev. D **100**(7), 073008 (2019). https://doi.org/10.1103/PhysRevD.100.073008
20. L. Hayen, Standard Model $\mathcal{O}(\alpha)$ renormalization of g_A and its impact on new physics searches. Phys. Rev. D **103**(11), 113001 (2021). https://doi.org/10.1103/PhysRevD.103.113001
21. M. Gorchtein, C.Y. Seng, Dispersion relation analysis of the radiative corrections to g_A in the neutron β-decay. J. High Energy Phys. **2021**(10), 53 (2021). https://doi.org/10.1007/JHEP10(2021)053
22. D.B. Kaplan, M.J. Savage, M.B. Wise, Nucleon-nucleon scattering from effective field theory. Nucl. Phys. B **478**, 629–659 (1996). https://doi.org/10.1016/0550-3213(96)00357-4
23. D.B. Kaplan, M.J. Savage, M.B. Wise, A New expansion for nucleon-nucleon interactions. Phys. Lett. B **424**, 390–396 (1998). https://doi.org/10.1016/S0370-2693(98)00210-X
24. D.B. Kaplan, M.J. Savage, M.B. Wise, Two nucleon systems from effective field theory. Nucl. Phys. B **534**, 329–355 (1998). https://doi.org/10.1016/S0550-3213(98)00440-4
25. U. van Kolck, Effective field theory for short-range forces. Nucl. Phys. A **645**(2), 273–302 (1999). https://doi.org/10.1016/S0375-9474(98)00612-5
26. J.W. Chen, G. Rupak, M.J. Savage, Nucleon-nucleon effective field theory without pions. Nucl. Phys. A **653**, 386–412 (1999). https://doi.org/10.1016/S0375-9474(99)00298-5
27. S.R. Beane, P.F. Bedaque, W.C. Haxton, D.R. Phillips, M.J. Savage, From hadrons to nuclei: crossing the border, in *At The Frontier of Particle Physics: Handbook of QCD* (2001), pp. 133–269. https://doi.org/10.1142/9789812810458_0011
28. G. Rupak, Precision calculation of np$\rightarrow$ dγ cross section for big-bang nucleosynthesis. Nucl. Phys. A **678**(4), 405–423 (2000). https://doi.org/10.1016/S0375-9474(00)00323-7
29. P.F. Bedaque, U. van Kolck, Effective field theory for few nucleon systems. Ann. Rev. Nucl. Part. Sci. **52**, 339–396 (2002). https://doi.org/10.1146/annurev.nucl.52.050102.090637
30. H.W. Hammer, S. König, U. van Kolck, Nuclear effective field theory: status and perspectives. Rev. Modern Phys. **92**(2), 025004 (2020). https://doi.org/10.1103/RevModPhys.92.025004
31. M.E. Luke, A.V. Manohar, I.Z. Rothstein, Renormalization group scaling in nonrelativistic QCD. Phys. Rev. D **61**(7), 074025 (2000). https://doi.org/10.1103/PhysRevD.61.074025
32. W.E. Caswell, G.P. Lepage, Effective Lagrangians for bound state problems in QED, QCD, and other field theories. Phys. Lett. B **167**(4), 437–442 (1986). https://doi.org/10.1016/0370-2693(86)91297-9
33. E. Epelbaum, H.W. Hammer, U.G. Meißner, Modern theory of nuclear forces. Rev. Modern Phys. **81**(4), 1773–1825 (2009). https://doi.org/10.1103/RevModPhys.81.1773

34. E. Epelbaum, H. Krebs, P. Reinert, High-precision nuclear forces from chiral EFT: State-of-the-art, challenges and outlook (2019). arXiv: 1911.11875
35. E. Epelbaum, H. Krebs, P. Reinert, Semi-local nuclear forces from chiral EFT: State-of-the-art & challenges (2022). arXiv: 2206.07072
36. R. Machleidt, D.R. Entem, Chiral effective field theory and nuclear forces. Phys. Rep. **503**(1), 1–75 (2011). https://doi.org/10.1016/j.physrep.2011.02.001
37. C.A. Bertulani, H.W. Hammer, U. van Kolck, Effective field theory for halo nuclei: shallow p-wave states. Nucl. Phys. A **712**(1–2), 37–58 (2002). https://doi.org/10.1016/S0375-9474(02)01270-8
38. H.W. Hammer, Theory of Halo Nuclei (2022). https://doi.org/10.48550/arXiv.2203.13074
39. H.W. Hammer, C. Ji, D.R. Phillips, Effective field theory description of halo nuclei. J. Phys. G Nucl. Part. Phys. **44**(10), 103002 (2017). https://doi.org/10.1088/1361-6471/aa83db
40. C.Y. Seng, M. Gorchtein, Towards ab initio nuclear theory calculations of δC (2023). arXiv: 2304.03800
41. I.S. Towner, J.C. Hardy, An improved calculation of the isospin-symmetry-breaking corrections to superallowed Fermi beta decay. Phys. Rev. C **77**(2), 025501 (2008). https://doi.org/10.1103/PhysRevC.77.025501
42. G.A. Miller, A. Schwenk, Isospin-symmetry-breaking corrections to superallowed Fermi beta decay: Formalism and schematic models. Phys. Rev. C **78**(3), 035501 (2008). https://doi.org/10.1103/PhysRevC.78.035501
43. M. Gorchtein, C.Y. Seng. Superallowed nuclear beta decays and precision tests of the Standard Model (2023). arXiv: 2311.00044
44. R.B. Wiringa, V.G.J. Stoks, R. Schiavilla, Accurate nucleon-nucleon potential with charge-independence breaking. Phys. Rev. C **51**(1), 38–51 (1995). https://doi.org/10.1103/PhysRevC.51.38
45. A. Tumino, G.G. Rapisarda, M. La Cognata, A. Oliva, A. Kievsky, C.A. Bertulani, G. D'Agata, M. Gattobigio, G.L. Guardo, L. Lamia, D. Lattuada, R.G. Pizzone, S. Romano, M.L. Sergi, R. Spartá, M. Viviani, Coulomb-free 1S0 p-p scattering length from the quasi-free p + d $\rightarrow$ p + p + n reaction and its relation to universality. Commun. Phys. **6**(1), 1–9 (2023). https://doi.org/10.1038/s42005-023-01221-0
46. P. Labelle, Effective field theories for QED bound states: extending Nonrelativistic QED to study retardation effects. Phys. Rev. D **58**(9), 093013 (1998). https://doi.org/10.1103/PhysRevD.58.093013. arxiv:hep-ph/9608491
47. B. Grinstein, I.Z. Rothstein, Effective field theory and matching in non-relativistic Gauge theories. Phys. Rev. D **57**(1), 78–82 (1998). https://doi.org/10.1103/PhysRevD.57.78. arxiv:hep-ph/9703298
48. M. Luke, M.J. Savage, Power counting in dimensionally regularized NRQCD. Phys. Rev. D **57**(1), 413–423 (1998). https://doi.org/10.1103/PhysRevD.57.413. arxiv:hep-ph/9707313
49. M. Luke, A.V. Manohar, Bound states and power counting in effective field theories. Phys. Rev. D **55**(7), 4129–4140 (1997). https://doi.org/10.1103/PhysRevD.55.4129. arxiv:hep-ph/9610534
50. H.W. Griesshammer, Threshold expansion and dimensionally regularised NRQCD. Phys. Rev. D **58**(9), 094027 (1998). https://doi.org/10.1103/PhysRevD.58.094027. arxiv:hep-ph/9712467
51. H.W. Griesshammer, Power counting and β function in NRQCD. Nucl. Phys. B **579**(1–2), 313–351 (2000). https://doi.org/10.1016/S0550-3213(99)00325-9. arxiv:hep-ph/9810235
52. A.V. Manohar, J. Soto, I.W. Stewart, The renormalization group for correlated scales: one-stage versus two-stage running. Phys. Lett. B **486**(3), 400–405 (2000). https://doi.org/10.1016/S0370-2693(00)00788-7
53. A.V. Manohar, I.W. Stewart, Logarithms of α in QED bound states from the renormalization group. Phys. Rev. Lett. **85**(11), 2248–2251 (2000). https://doi.org/10.1103/PhysRevLett.85.2248
54. X. Kong, F. Ravndal, Coulomb effects in low energy proton-proton scattering. Nucl. Phys. A **665**(1–2), 137–163 (2000). https://doi.org/10.1016/S0375-9474(99)00406-6. arxiv:hep-ph/9903523
55. T. Mehen, I.W. Stewart, Radiation pions in two-nucleon effective field theory. Nucl. Phys. A **665**(1–2), 164–182 (2000). https://doi.org/10.1016/S0375-9474(99)00368-1
56. D.B. Kaplan, M.J. Savage, M.B. Wise, A perturbative calculation of the electromagnetic form factors of the deuteron. Phys. Rev. C **59**(2), 617–629 (1999). https://doi.org/10.1103/PhysRevC.59.617
57. S. Weinberg, *The Quantum Theory of Fields: Volume 1: Foundations*, vol. 1 (Cambridge University Press, Cambridge, 1995). https://doi.org/10.1017/CBO9781139644167
58. J.J. de Swart, C.P.F. Terheggen, V.G.J. Stoks. The low-energy neutron-proton scattering parameters and the deuteron (1995). arXiv: nucl-th/9509032

Publisher's Note Springer Nature remains neutral with regard to jurisdictional claims in published maps and institutional affiliations.